Helicopter Maneuver Trajectory Tracking Control Based on Implicit Model and LADRC

REN Binwu[1], *CUI Zhuangzhuang*[1], *XU Yousong*[1], *DU Siliang*[2*], *ZHAO Qijun*[1*]

1. National Key Laboratory of Helicopter Aeromechanics, Nanjing University of Aeronautics and Astronautics, Nanjing 210016, P. R. China; 2. Faculty of Mechanical & Material Engineering, Huaiyin Institute of Technology, Huaian 223003, P. R China

(Received 18 January 2024; revised 24 Sepember 2024; accepted 15 October 2024)

Abstract: To enhance the stability of helicopter maneuvers during task execution, a composite trajectory tracking controller design based on the implicit model (IM) and linear active disturbance rejection control (LADRC) is proposed. Initially, aerodynamic models of the main and tail rotor are created using the blade element theory and the uniform inflow assumption. Subsequently, a comprehensive flight dynamic model of the helicopter is established through fitting aerodynamic force fitting. Subsequently, for precise helicopter maneuvering, including the spiral, spiral up, and Ranversman maneuver, a regular trim is undertaken, followed by minor perturbation linearization at the trim point. Utilizing the linearized model, controllers are created for the IM attitude inner loop and LADRC position outer loop of the helicopter. Ultimately, a comparison is made between the maneuver trajectory tracking results of the IM-LADRC and the conventional proportional-integral-derivative (PID) control method is performed. Experimental results demonstrate that utilizing the post-trim minor perturbation linearized model in combination with the IM-LADRC method can achieve higher precision in tracking results, thus enhancing the accuracy of helicopter maneuver execution.

Key words: helicopter; trajectory tracking; implicit model (IM); proportional-integral-derivative (PID); linear active disturbance rejection control; small disturbance linearization; spiral up; Ranversman maneuver

CLC number: V249.1 **Document code:** A **Article ID:** 1005-1120(2024)06-0739-11

0 Introduction

Due to their high degree of mobility, helicopters are extensively utilized in both military and civilian sectors[1]. The implementation of trajectory tracking for the maneuvers executed by these vehicles significantly aids pilots in completing a variety of strategic movements. Considering the numerous external factors that influence helicopter navigation, the stability of the control system is of paramount importance[2]. Among its components, attitude control is vital for system stability and serves as the foundation for maintaining a helicopter's steady flight[3].

For the design of controllers for trajectory tracking, the classic proportional-integral-derivative (PID) feedback control theory offers clear advantages due to its simplistic algorithm, feasibility for engineering implementation, and the evident physical significance of parameter adjustment[4]. However, its efficacy falls short in the context of multi-input multi-output (MIMO) systems. The limitations of classical control led to the emergence of modern control theory. Modern control theories are based on the state space method. The research object includes solving complex multi-input multi-output systems, but the model accuracy requirements are high[5]. Active disturbance rejection control plays the advantages of PID, maintains the control strategy of error elimination by error, and overcomes defects. PID corresponds to the error that has been generated to eliminate it, and active disturbance re-

*Corresponding authors, E-mail addresses: dusl_aircraft@nuaa.edu.cn, zhaoqijun@nuaa.edu.cn.

How to cite this article: REN Binwu, CUI Zhuangzhuang, XU Yousong, et al. Helicopter maneuver trajectory tracking control based on implicit model and LADRC[J]. Transactions of Nanjing University of Aeronautics and Astronautics, 2024, 41(6):739-749.

http://dx.doi.org/10.16356/j.1005-1120.2024.06.006

jection control eliminates the factors that cause the error before the large error occurs[6].

Helicopters serve as the epitome of multi-input and multi-output systems[7]. Therefore, it is evident that the sole implementation of PID feedback control cannot produce optimal control results. To satisfy the requirements of flight control performance, extensive research has been undertaken on the suitability of alternative controller designs in engineering. For instance, Wu et al.[8], among others, successfully circumnavigated quadrotor flight models' rampant non-linearity and intense interlinking issues through the backing step method, subsequently achieving trajectory control. Xian et al.[9] adopted the sliding mode control in tracking helicopters' preset speed and yaw trajectory. In response to the instability, non-linearity, and severe coupling of small unmanned aircraft, Ding et al.[10] proposed a trajectory-tracking method with inherent disturbance rejection. Both sliding mode control and disturbance rejection have demonstrated effective results in helicopter trajectory tracking, although the latter has demonstrated superior robustness. The disturbance rejection controller technology requires low dependency on system models and can efficaciously handle internal and external disturbances[11-14]. In this paper, the focus is on trajectory tracking during the maneuvers of the UH-60 helicopter. Given the helicopter's non-linearity and strong coupling characteristics[15], a high-robustness method is imperative.

We first establish the nonlinear full-fledged aerodynamic model for the UH-60 helicopter. Following this, the model is used as the basis to trim the helicopters under varying states to achieve stable controls and attitudes. Near the stable state, small perturbation linearization is applied to derive the linearized model. Based on this linear model, implicit model (IM) is used to decouple the attitude of the helicopter's inner loop. This approach solves the problem of strong coupling in the model and simplifies the complexity of the model. Linear active disturbance rejection control (LADRC) realizes the attitude stability control of the inner loop based on IM decoupling and solves the problem of poor control effect of the outer loop controller caused by the instability of the inner loop. Finally, LADRC estimates and compensates for the disturbance error of the outer loop based on the stable inner loop to realize the final position tracking, which suppresses the influence of model error and external disturbance on the trajectory controller. Ultimately, the research conducts trajectory tracking simulation control on the UH-60 helicopter for three classic maneuvers: hovering, ascending in hover, and performing the Ranversman maneuver. The tracking performance is compared with controls driven by the traditional PID method to validate the methodology proposed in this paper.

1 Establishment of Helicopter Dynamics Model

1.1 Whole aircraft dynamics model and trim method

The research object of this paper is the UH-60 helicopter. Its aerodynamic characteristics are poor stability and serious coupling between longitudinal and lateral channels[16]. To construct the aerodynamic model of the whole aircraft, this paper divides the rotor, tail rotor, fuselage, horizontal and vertical tail parts to establish the aerodynamic model of the whole aircraft. For the rotor, the blade flapping motion is calculated using the rigid body flapping model, and then the induced velocity and aerodynamic force are calculated by using the momentum-blade element theory and the aerodynamic model is established. For the tail rotor, the momentum-blade element method is also used to calculate, and the aerodynamic forces of the fuselage and the vertical tail are fitted by formulas. The flight dynamics model of the whole aircraft is constructed by combining the six-degree-of-freedom equations of the rigid body[17]. The nonlinear multi-input multi-output model of the Black Hawk helicopter has been obtained. Its nonlinear total motion equation is

$$\dot{\boldsymbol{x}}=f(\boldsymbol{x},\boldsymbol{u}_c,t) \tag{1}$$

where $\boldsymbol{x}=(u,v,w,p,q,r,\phi,\theta,\psi)$, and $u,v,w,p,q,r,\phi,\theta,$ and ψ are the helicopter state variables of forward speed, lateral speed, vertical speed, roll angle rate, pitch angle rate, yaw angle rate, roll angle, pitch angle and yaw angle, respectively; $\boldsymbol{u}_c=(\delta_c, \delta_a, \delta_e, \delta_r)$, and δ_c, δ_a, δ_e, and δ_r are the inputs of rotor collective pitch, lateral periodic pitch, longitudinal periodic pitch and tail rotor collective pitch, respectively.

After establishing the aerodynamic model of the whole helicopter, the Newton iteration method is used to trim the helicopter[18]. The UH-60 helicopter modeling data are shown in Table 1.

Table 1 Basic parameters of UH60

Parameter	Value
Gross mass/kg	7 258
Centre of gravity position/m	(−8.9, 0, −5.9)
Rotor radius/m	8.18
Rotor speed/(rad•s^{-1})	27
Number of rotor blades	4
Forward tilt angle of rotor shaft/(°)	3
Waving hinge extension of rotor blade/m	0.381
Average chord length of rotor blade/m	0.527
Rotor blade torsion/(°)	−10.9
Rotor position/m	(−8.67, 0, −8)
Inertia moment of fuselage around X axis/(kg•m^2)	7 406.156
Inertia moment of fuselage around Y axis/(kg•m^2)	50 012.28
Inertia moment of fuselage around Z axis/(kg•m^2)	53 512.55
Inertia product of fuselage in XOY plane/(kg•m^2)	2 133.831
Tail rotor radius/m	1.68
Tail rotor speed/(rad•s^{-1})	124.62
Average chord length of tail rotor/m	0.247
Number of tail rotor blades	4
Negative torsion of tail rotor	−18

The main trimming process of the Newton iterative method is shown in Fig.1, and the steps are as follows.

Step 1 Determine the maximum number of iteration steps N, the convergence value e, and the initial input of the trim x_0.

Step 2 The aerodynamic force of the whole helicopter is calculated by the helicopter aerodynamic model and incorporated into the equilibrium equations to calculate $F(x_0)$. The Jacobian matrix $F'(x_0)$ of the equilibrium equations is calculated by the difference quotient method. Determine whether the Jacobian matrix is singular. If singular, the output matrix is singular and the trim failure identification is output. If non-singular, the next step is performed.

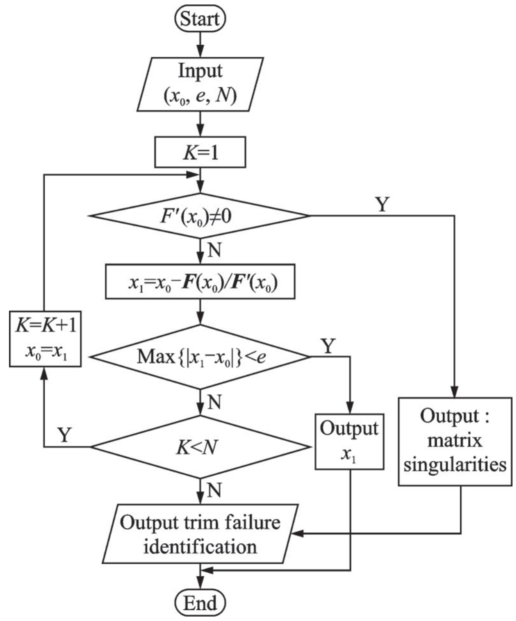

Fig.1 Flow chart of Newton iterative method

Step 3 The step length of the trim is obtained by multiplying the calculated aerodynamic force of the whole aircraft by the inverse of the Jacobian matrix.

Step 4 According to the step size to determine the next step of the trim value x_1, to determine whether the value of the maximum step size in the two trim values is less than the convergence value e, if less than the output x_1 as a trim, if not less than the next step.

Step 5 To determine if the number of trim calculation steps M at this time is less than the maximum number of trim steps N, if so, let the number of trim steps M add the value of x_1 to x_0 and proceed to the second step. If not, the output trim failure identification.

According to the verification of the trim of the calculation results in this paper, as shown in Fig.2, the change of the control quantity and attitude angle with the forward flight speed is in good agreement with the experimental values when the forward flight trim is carried out. The aerodynamic model and trim method outlined in this paper can be utilized to determine the stable state of the helicopter when the small disturbance is linearized.

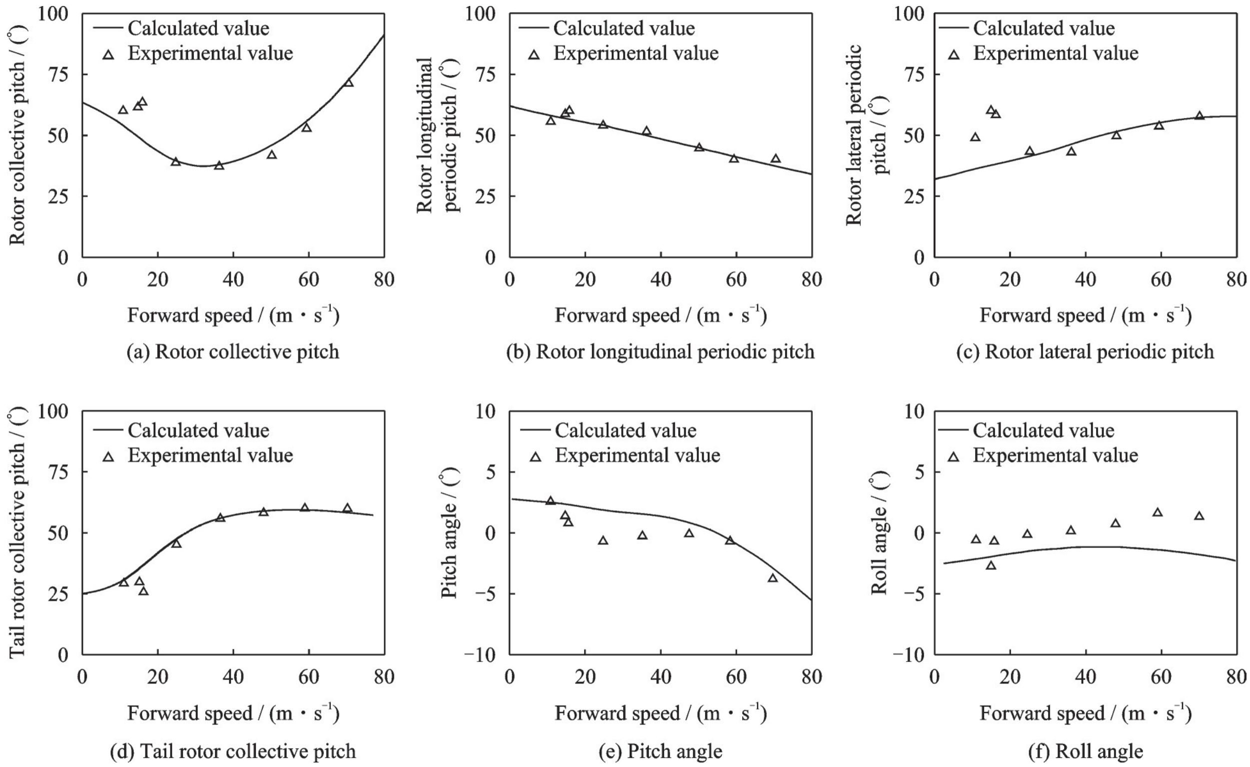

Fig.2 Comparison between trim value and experimental value in this paper

1.2 Small disturbance linearization model

To obtain a reasonable helicopter linear model, this paper first discretizes the typical profile for the state that needs to be controlled, and then performs quasi-steady state trim on the discrete points to obtain the corresponding trim state. The small disturbance linearization model is obtained by adding small disturbance to the trim state. It can be assumed that the state equation of the helicopter after small disturbance linearization is

$$\Delta\dot{\boldsymbol{x}} = \boldsymbol{A}\Delta\boldsymbol{x} + \boldsymbol{B}\Delta\boldsymbol{u} \tag{2}$$

where Δ represents the small disturbance variation, and $\boldsymbol{A}$ and $\boldsymbol{B}$ represent the coefficient matrix and the control matrix, respectively.

The coefficient in the system control matrix $\boldsymbol{B}$ represents the control derivative, and the coefficient in the state matrix $\boldsymbol{A}$ is the stability derivative. The helicopter's flight state determines its numerical change. From the helicopter dynamics model, it can be seen that the coupling of the helicopter is manifested by the state matrix $\boldsymbol{A}$ (dynamic coupling) and the control matrix $\boldsymbol{B}$ (control coupling).

2 Trajectory Tracking Controller Structure

2.1 Implicit model controller

The essence of IM control is to embed the desired attitude inner-loop response characteristics in an implicit model, which must meet the response characteristics required by the helicopter and reflect its decoupling requirements. Based on the classic inner-outer loop feedback control structure, this paper will design the helicopter control law. The IM controller's inner loop for helicopter attitude is shown in Fig.3.

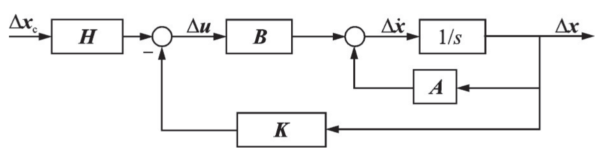

Fig.3 Inner loop structure configuration of hidden model controller

In Fig.3, an implicit model method is used to design the state feedback matrix $\boldsymbol{K}$ and the feedforward compensation matrix $\boldsymbol{H}$, so the expected closed-loop response characteristics are as follows

$$\Delta\dot{\boldsymbol{x}} = \boldsymbol{A}^{\mathrm{d}}\Delta\boldsymbol{x} + \boldsymbol{B}^{\mathrm{d}}\Delta\boldsymbol{x}_{\mathrm{c}} \tag{3}$$

where $\Delta \boldsymbol{x}_c$ is the control variable of the controller, $\boldsymbol{A}^d$ the desired state matrix, and $\boldsymbol{B}^d$ the desired control matrix. It can be seen from the control structure

$$\begin{cases} \boldsymbol{A}^d = \boldsymbol{A} - \boldsymbol{BK} \\ \boldsymbol{B}^d = \boldsymbol{BH} \end{cases} \tag{4}$$

Then the state feedback matrix $\boldsymbol{K}$ and the feed-forward compensation matrix $\boldsymbol{H}$ can be obtained as

$$\begin{cases} \boldsymbol{K} = \boldsymbol{B}(\boldsymbol{A} - \boldsymbol{A}^d) \\ \boldsymbol{H} = \boldsymbol{B}^{-1}\boldsymbol{B}^d \end{cases} \tag{5}$$

After decoupling through the state feedback matrix $\boldsymbol{K}$ and the feed-forward compensation matrix $\boldsymbol{H}$, the inner loop can be approximated as independent channels. On this basis, the structure of the position outer loop is designed.

2.2 Linear active disturbance rejection controller

The LADRC controller operates by responding to disturbances that act on the control object, leading to the generation of errors[19]. It is a controller that detects and corrects errors. The main concept is to actively extract disturbance information from the input and output signal values of the controlled object and utilize the control signal to eliminate it promptly[20]. The LADRC controller compensates for the residual coupling between each inner loop channel and the external disturbances (unknown factors) as total system disturbances[21]. The LADRC structure is shown in Fig.4. The active disturbance rejection controller in Fig.4 mainly includes the linear tracking differentiator (LTD), the linear extended state observer (LESO), and the linear state error feedback (LSEF).

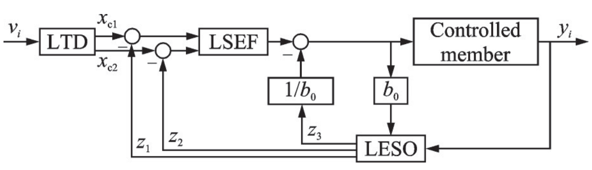

Fig.4 Structure diagram of LADRC

The LTD is used to extract the differential signal by tracking the given signal as quickly as possible and can resolve the conflict between overshoot and rapidity[22]. It arranges the appropriate signal transition process according to the bearing capacity of the system. The discrete form of the LTD is

$$\begin{cases} x_{c1}(t+1) = x_{c1}(t) + h \cdot x_{c2}(t+1) \\ x_{c2}(t+1) = x_{c2}(t) + h \cdot (-r^2(x_{c1} - x) - 2rx_{c2}) \end{cases} \tag{6}$$

where t is the number of sampling, x the input signal, x_{c1} the tracking signal of the input signal, x_{c2} the differential signal of x_{c1}, h the sampling step size, and r the speed factor that determines the tracking speed (according to the transition speed requirement and the system's bearing capacity).

The LESO is the part of the active disturbance rejection controller. It can affect the disturbance effect of the controlled object output by expanding into a new state variable. A special feedback mechanism is used to establish a state that can be observed and expanded. It does not depend on the specific mathematical model of the generated disturbance. It is mainly used to estimate the synthesis of internal and external disturbances acting on the system in real time and compensate them[23]. The extended state observer is mainly divided into the nonlinear state error server (NLESO) and LESO. NLESO has the advantages of high parameter efficiency and high tracking accuracy, but its tracking performance is related to the disturbance amplitude, and its ability to estimate large disturbance is limited. The tracking performance of LESO does not change with the disturbance amplitude[24]. The working environment of the helicopter is greatly disturbed, so the specific form of LESO is selected as

$$\begin{cases} e = z_1(t) - y \\ z_1(t+1) = z_1(t) + h(z_2(t) - \beta_{01}e) \\ z_2(t+1) = z_2(t) + h(z_3(t) - \beta_{02}e + b_0 u) \\ z_3(t+1) = z_3(t) + h(-\beta_{03}e) \end{cases} \tag{7}$$

where b_0 is the compensation factor; z_1, z_2, and z_3 are the tracking value and differential signal of the system output, and β_{01}, β_{02}, and β_{03} the gain parameters of the observer determined by the sampling step size of the system. The concept of bandwidth is used to determine the observer parameters as[25]

$$\beta_{01} = 3\omega_0, \beta_{02} = 3\omega_0^2, \beta_{03} = \omega_0^3 \tag{8}$$

Eq.(8) simplifies the gain parameter of the observer to a parameter related to the bandwidth ω_0. Generally, the bandwidth ω_0 has a wide range of adaptation, and the bandwidth ω_0 suitable for the system can be selected.

The LSEF expression is

$$\begin{cases} e_1 = x_{c1} - z_1 \\ e_2 = x_{c2} - z_2 \\ u_0 = k_1 e_1 + k_2 e_2 \end{cases} \tag{9}$$

where k_1 and k_2 are the controller gains. They are determined by the concept of controller bandwidth as

$$k_1 = \omega_c^2,\ k_2 = 2\xi\omega_c \tag{10}$$

where ω_c is the natural frequency required for the closed-loop system, and ξ the damping ratio to avoid system oscillation.

The total control amount of the active disturbance rejection controller is

$$u = \frac{u_0 - z_3}{b_0} \tag{11}$$

where b_0 is the compensation factor.

2.3 Inner and outer loop controller structure

The trajectory tracking controller structure designed in this paper includes an attitude loop and a position loop. The attitude loop is composed of a LADRC and IM composite controller. The IM controller is used to control the initial decoupling of the object model. LADRC is used to eliminate the error effects caused by disturbances and achieve stable responses in each attitude channel. The position loop achieves a stable response of the position channel through LADRC, ultimately enabling tracking of the desired trajectory. Combining the above methods, the final structure of the controller can be obtained, as shown in Fig.5.

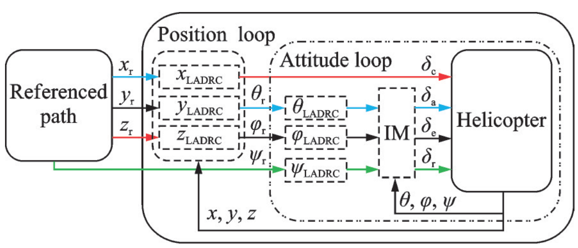

Fig.5 Overall structure diagram of the controller

After decoupling the control matrix, the closed-loop response characteristics of the state equation are shown in Eq.(7). The control input can be determined as

$$\begin{bmatrix} U_1 \\ U_2 \\ U_3 \end{bmatrix} = B^d(t) \begin{bmatrix} u_1 \\ u_2 \\ u_3 \end{bmatrix} \tag{12}$$

The above control quantity corresponding to the active disturbance rejection controller algorithm is organized as

$$\begin{cases} x_{ic1}(t+1) = x_{ic1}(t) + h \cdot x_{ic2}(t+1) \\ x_{ic2}(t+1) = x_{ic2}(t) + h \cdot (-r^2(x_{ic1} - x) - 2rx_{ic2}) \\ e = z_{i1}(t) - y \\ z_{i1}(t+1) = z_{i1}(t) + h(z_{i2}(t) - \beta_{01} e) \\ z_{i2}(t+1) = z_{i2}(t) + h(z_{i3}(t) - \beta_{02} e + b_0 u) \\ z_{i3}(t+1) = z_{i3}(t) + h(-\beta_{03} e) \\ e_1 = x_{ic1} - z_{i1},\ e_2 = x_{ic2} - z_{i2} \\ u_{i0} = k_1 e_1 + k_2 e_2 \\ u_i = \dfrac{u_0 - z_{i3}}{b_0} \end{cases} \tag{13}$$

The four-channel final control quantity of the helicopter attitude controller is (U_1, U_2, U_3) in Eq.(12). The controller parameters to be adjusted are the sampling step size h, the speed factor r, the bandwidth ω_0, the natural frequency ω_c required for the closed-loop system and the compensation factor b_0, where r is determined according to the transition speed requirement and the system's bearing capacity, and h is the sampling step size of the system.

3 Simulation and Result Analysis

To verify the control method used in this paper, the mathematical model of UH-60 is used to build the mathematical model and the designed controller in the Simulink environment. The PID parameters (P, I, D) are shown in Table 2, and the parameters of the LADRC are shown in Table 3.

Table 2 PID trajectory tracking controller parameters

Parameter	Roll angle	Pitch angle	Yaw angle	X	Y	Z
P	1.5	2.0	1.00	1.3	1.2	0.6
I	0.2	0.1	0.10	0.3	0.1	0
D	0.1	0.2	0.15	0.1	0.1	0

Table 3 LADRC trajectory tracking controller parameters

Parameter	Roll angle	Pitch angle	Yaw angle	X	Y	Z
ω_0	25	22	20	10	8	10
ω_c	12	12	10	5	5	3
b_0	5	6	5	2	1	1

3.1 Attitude loop simulation analysis

The parameters for the PID and LADRC attitude loops, displayed in Tables 1, 2, allow comparative analysis of the response speeds, disturbance resistance, and robustness of various channels.

Evaluating the response speed of the control methods under the parameters in Table 1, without disturbances or model errors, the set roll angle, pitch angle, and yaw angle targets are all identified as step signals of 5°. At 5 s, the expected target attitude shifts to $-5°$. For the comparative analysis, the stabilization and efficiency of the PID and IM-LADRC controllers are considered, with a simulation providing the results as presented in Fig.6. It is evident that the designed IM-LADRC controller stabilizes tracking in a brief period, its response speed surpassing traditional PID controllers and IM controllers. Even after a change in target expectation tracking at 5 s, the IM-LADRC controller continues to track the target attitude swiftly and without overshooting. This proves the rapidity and stability of the IM-LADRC controller are superior to those of the IM controller and PID controller.

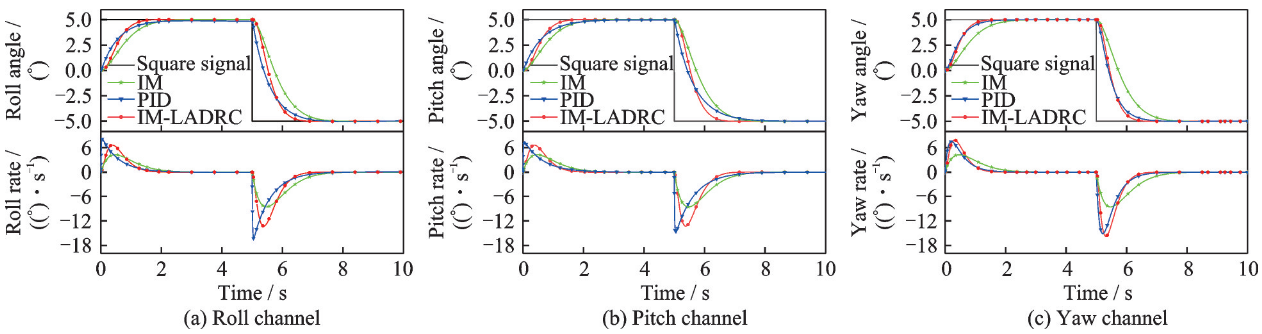

Fig.6 Rapid simulation

In assessing the robustness of the control methods, this study, based on a square wave signal simulation experiment, assumes a 50% modeling error in comparison with the actual model. The robustness results of the IM, PID, and IM-LADRC controllers are compared, with the simulation outcomes depicted in Fig.7. As illustrated in Fig.7, the IM controller's attitude angle tracking signal proves inaccurate and experiences significant fluctuations when errors are present in the linearized model, underlining the substantial impact of model accuracy on the IM controller. Both the IM-LADRC controller and PID controller can stabilize tracking in a short timeframe, albeit, even the PID controller is susceptible to fluctuations. This evidence corroborates that IM-LADRC controller demonstrates low model dependency and superior robustness.

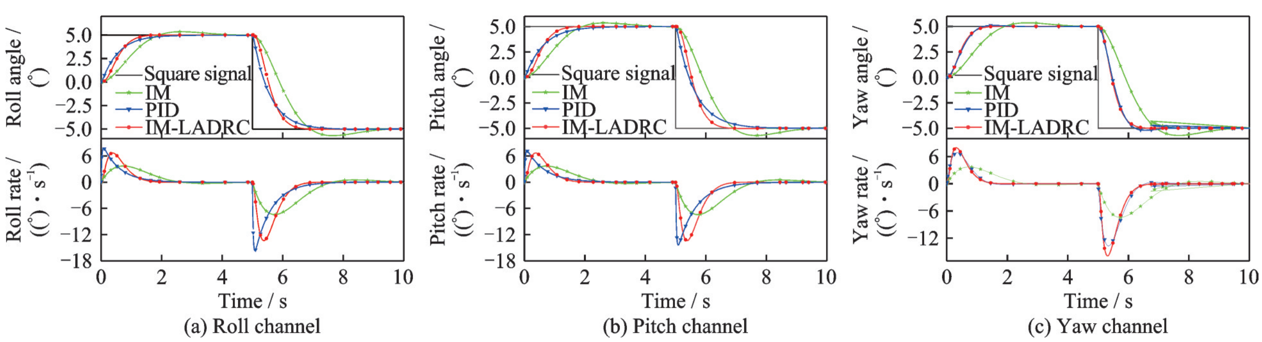

Fig.7 Robustness simulation

Helicopters are susceptible to external disturbances during flight. Consequently, within the controller's attitude angle rate loop, vertical speed, and attitude angle speed measurement signals. The noise disturbances are added, featuring a sampling rate of 100 Hz and an average amplitude of 4°. This process simulated the influence of noise signals on the helicopter's performance. The disturbance rejection capabilities of IM, PID, and IM-LADRC controllers were compared and analyzed, with the simulation outcomes visualized in Fig. 8. The results indicate that under noise signal interference, the IM controller's attitude angle of the IM controller shows significant oscillation. In contrast, the oscillation amplitude of the IM-LADRC and PID attitude angles is approximately $\pm 0.2°$ and $\pm 2°$, respectively. Hence, the disturbance rejection ability of the IM-LADRC controller is significantly superior to both the IM controller and PID controller.

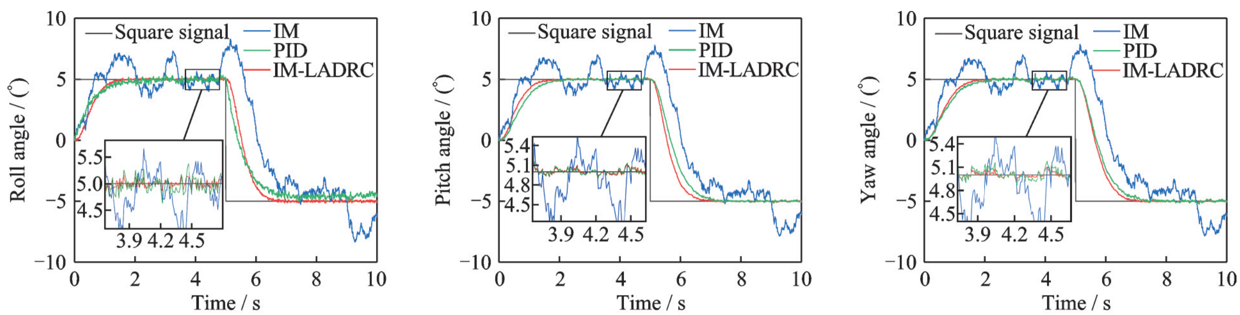

(a) Roll channel (b) Pitch channel (c) Yaw channel

Fig.8 Immunity simulation

The results from the preceding three simulations indicate that the IM-LADRC controller surpasses both the PID controller and the IM controller in terms of stability, robustness, and immunity to disturbance. The rationale behind this can be expanded upon as follows:

(1) The IM-LADRC controller decouples the high-order coupling system into single-input and single-output. It treats external disturbances and the coupling of state quantities as perturbations to be eliminated. Hence, the IM-LADRC controller demonstrates excellent traceability and prompt response time.

(2) In cases where the controlled object contains modeling errors, such errors may alter the internal response characteristics of the IM, thereby affecting system stability. The IM-LADRC controller treats modeling errors as internal disturbances to the system, thereby ensuring greater robustness.

(3) When the controlled object is subjected to noise signal interference, both the IM-LADRC and PID controllers treat the noise signals as external disturbances to be eliminated. However, the IM-LADRC controller tuned with optimal parameters exhibits superior disturbance rejection capabilities and lower fluctuations, making it superior to both the IM and PID controllers in terms of resilience to disturbances.

3.2 Spiral trajectory tracking

Helicopter hovering plays a significant role in executing aerial observation tasks and air traffic control rescue tasks during the flight journey of the helicopter. Hovering refers to a helicopter maintaining a relatively stable position around a vertical or horizontal axis with a single point as the center, all while rotating around this point. This is a relatively simple helicopter maneuver, with state changes requiring single solutions for both Array A and Array B under these circumstances. Utilizing the methodologies, this paper traces the trajectory of a hovering state in helicopters. Fig.9 presents the tracking status and trajectory results of the displacement coordinates in a helicopter during its hover ascent state. The PID controller has significant tracking errors and overshoot. The tracking accuracy of the hovering state achieved by the control method proposed in this paper is noticeably higher.

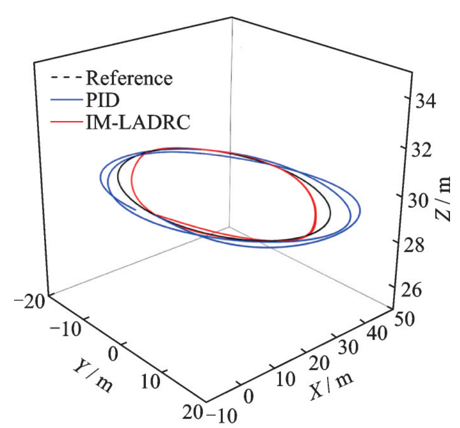

(a) Spiral trajectory tracking

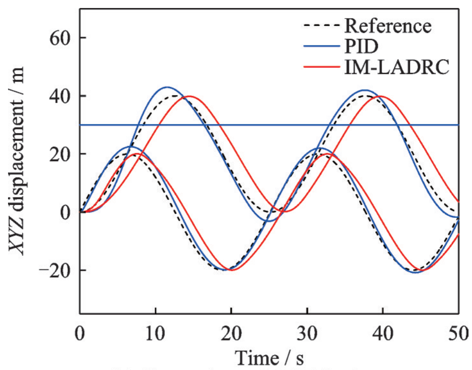

(b) Comparison of *XYZ* displacement

Fig.9 Trajectory tracking results of spiral

3.3 Spiral up trajectory tracking

The ability of a helicopter to ascend while hovering is crucial for maintaining the flexibility of manoeuvres, broadening the helicopter's field of view, and adjusting its height without losing track of the target. This manoeuvre involves the gradual elevation of the helicopter while it is executing a hover, also called a hover ascent. This study utilizes the aforementioned methodologies to trace the trajectory of a hovering state in helicopters. Fig.10 displays the displacement coordinate tracking and trajectory results of a helicopter in a hover ascent state. Notably, the tracking line appears deviated, and the PID, similar to that in hover, has a significant overshoot. The methodology employed in this study performs better in tracking the trajectory of a helicopter's hover ascent with less error.

3.4 Ranversman maneuvering trajectory tracking

The Ranversman maneuver implemented in helicopters allows for swift strike and re-strike on ground targets. The maneuver first involves a rapid ascent of the helicopter, followed by a 180° inversion and subsequent downward dive when the helicopter reaches its peak and nears a speed of zero. This document traces the consecutive Ranversman actions of the helicopter, which exhibit a saddle-shaped trajectory at this point. The final tracking results, as illustrated in Fig.11, show that the use of the method IM-LADRC employed in this study carries a higher degree of tracking precision, thereby enabling the effective tracking of the Ranversman maneuver trajectory. The PID tracking performance, in contrast, is poor, with a significant overshoot causing deformation of the traced trajectory.

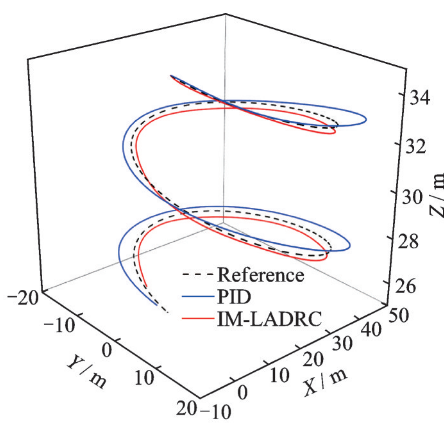

(a) Spiral up trajectory tracking

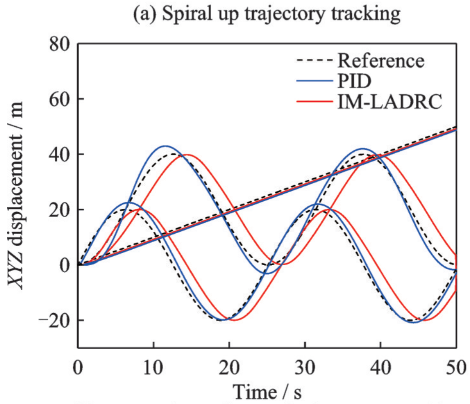

(b) Comparison of *XYZ* displacement tracking

Fig.10 Trajectory tracking results of spiral up

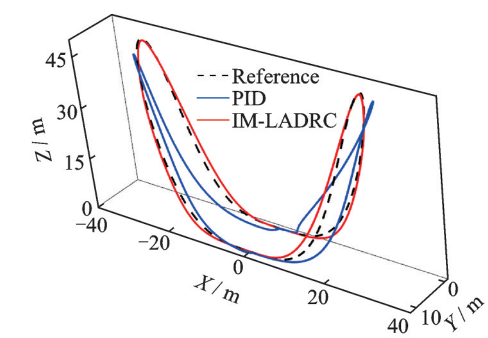

(a) Ranversman maneuvering trajectory tracking

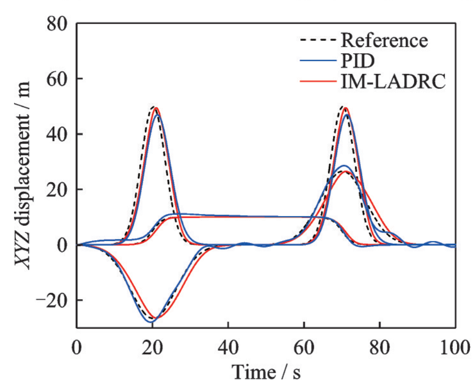

(b) Comparison of *XYZ* displacement tracking

Fig.11 Trajectory tracking results of Ranversman maneuvaring

4 Conclusions

This study constructs a full aircraft non-linear aerodynamic model and performs trim work for three types of helicopter maneuver actions. Small perturbations were linearized around the trim value, and a corresponding composite IM-LADRC controller was designed. Simulation of trajectory tracking for the helicopter's three maneuver actions was conducted and compared with traditional PID methods, leading to the following conclusions:

(1) Simulation verification demonstrates that the IM-LADRC controller's attitude loop, due to the IM's decoupling of the internal model, responds more rapidly to the input signals of the controlled object. In addition, the LADRC's timely estimation and compensation for the effects of external disturbances and internal model errors endow the composite controller with superior robustness and disturbance rejection capabilities.

(2) The IM-LADRC trajectory tracking controller demonstrates superior control performance in the inner-loop, and compared to PID methods, it achieves better tracking performance on the outer-loop trajectory. As a result, this composite controller exhibits greater robustness and higher tracking precision in tracking complex maneuvers.

References

[1] WANG S. Approximation-free control for nonlinear helicopters with unknown dynamics[J]. IEEE Transactions on Circuits and Systems Ⅱ: Express Briefs, 2022, 69(7): 3254-3258.

[2] YIN X, PENG X M, ZHANG G C, et al. Flight control system design and autonomous flight control of small-scale unmanned helicopter based on nanosensors[J]. Journal of Nanoelectronics and Optoelectronics, 2021, 16(4): 675-688.

[3] KHALESI M H, SALARIEH H, SAADAT F M. System identification and robust attitude control of an unmanned helicopter using novel low-cost flight control system[J]. Proceedings of the Institution of Mechanical Engineers, Part Ⅰ: Journal of Systems and Control Engineering, 2020, 234(5): 634-645.

[4] HAN Jinqing. From PID technique to active disturbances rejection control technique[J]. Control Engineering of China, 2002(3): 13-18. (in Chinese)

[5] WANG Chuanbo, LIU Yang. Comparative research of modern control theory and classical control theory[J]. Mechanical Management and Development, 2006(3): 6-8. (in Chinese)

[6] GAO Zhiqiang. On the foundation of active disturbance rejection control[J]. Control Theory & Applications, 2013, 30(12): 1498-1510. (in Chinese)

[7] THOMAS F, MIJA S J. Output feedback based adaptive composite nonlinear flight control design for a small-scale un-crewed helicopter[J]. ISA Transactions, 2022, 126: 190-202.

[8] WU K J, ZHANG P X, WU H. A new control design for a morphing UAV based on disturbance observer and command filtered backstepping techniques[J]. Science China (Technological Sciences), 2019, 62(10): 1845-1853.

[9] XIAN B, GUO J C, ZHANG Y, et al. Sliding mode tracking control for miniature unmanned helicopters[J]. Chinese Journal of Aeronautics, 2015, 28(1): 277-284.

[10] DING Shenping, WU Weirong, YU Shuang, et al. A trajectory tracking control of small-scale unmanned helicopters[J]. Computer Simulation, 2016, 33(11): 28-32. (in Chinese)

[11] SHEN S Y, XU J F. Adaptive neural network-based active disturbance rejection flight control of an unmanned helicopter[J]. Aerospace Science and Technology, 2021, 119: 107062.

[12] SHEN S Y, XU J F. Trajectory tracking active disturbance rejection control of the unmanned helicopter and its parameters tuning[J]. IEEE Access, 2021, 9: 56773-56785.

[13] ANG S, YANG Q H, QIAN S K, et al. Height and attitude active disturbance rejection controller design of a small-scale helicopter[J]. Science China Information Sciences, 2015, 58: 1-17.

[14] DING L, MA R, WU H, et al. Yaw control of an unmanned aerial vehicle helicopter using linear active disturbance rejection control[J]. Proceedings of the Institution of Mechanical Engineers, Part Ⅰ: Journal of Systems and Control Engineering, 2017, 231(6): 427-435.

[15] PENG M H, ZHANG C L. Optimization design of helicopter stability and control[J]. Journal of Nanjing University of Aeronautics & Astronautics, 2011, 43(3): 283-288. (in Chinese)

[16] QIN C, QIN N, LI R, et al. ADRC fractional order PID controller design of hypersonic flight vehicle[J]. Transactions of Nanjing University of Aeronautics & Astronautics, 2011, 28(3): 240-245.

[17] MENG W L, CHEN R L. Study of helicopter autorotation landing following engine failure based on a six-degree-of-freedom rigid-body dynamic model[J]. Chi-

nese Journal of Aeronautics, 2013, 26(6): 1380-1388.

[18] CUI Zhuangzhuang, YUAN Xin, ZHAO Guoqing, et al. Influence of control strategy on the forward flight performance of a coaxial rig-id rotor high-speed helicopter[J]. Acta Aeronautica et Astronautica Sinica, 2023, 45(9): 529256. (in Chinese)

[19] HAN Jinqing. Auto disturbances rejection control technique[J]. Frontier Science, 2007(1):24-31. (in Chinese)

[20] LI Jie, QI Xiaohui, WAN Hui, et al. Active disturbance rejection control: Theoretical results summary and future researches[J]. Control Theory & Applications, 2017, 34(3): 281-295. (in Chinese)

[21] LIU C Q, LUO G Z, DUAN X L, et al. Adaptive LADRC-based disturbance rejection method for electromechanical servo system[J]. IEEE Transactions on Industry Applications, 2019, 56(1): 876-889.

[22] HEZZI A, BEN E S, BENSALEM Y, et al. ADRC-based robust and resilient control of a 5-phase PMSM driven electric vehicle[J]. Machines, 2020, 8(2): 17.

[23] CHEN Zengqiang, CHENG Yun, SUN Mingwei, et al. Surveys on theory and engineering applications for linear active disturbance rejection control[J]. Information and Control, 2017, 46(3): 257-266. (in Chinese)

[24] LI Jie, QI Xiaohui, XIA Yuanqing, et al. On linear/nonlinear active disturbance rejection switching control[J]. Acta Automatica Sinica, 2016, 42(2): 202-212. (in Chinese)

[25] GAO Z Q. Scaling and bandwidth-parameterization based controller tuning[C]//Proceedings of the 2023 American Control Conference.[S.l.]: IEEE,2023.

Acknowledgements This work was supported in part by the National Natural Science Foundation of China (No.12032012); the Key Discipline Construction Project of Colleges and Universities in Jiangsu Province.

Authors Mr. **REN Binwu** is now a Ph. D. candidate in Nanjing University of Aeronautics and Astronautics (NUAA). His research direction is mainly related to helicopter flight control and intelligent control.

Prof. **DU Siliang** received his Ph.D. degree in fluid mechanics from NUAA in 2017. His main research direction is mainly engaged in research and development in the fields of UAV and robot system design and integration.

Prof. **ZHAO Qijun** received his Ph.D. degree in aerodynamics from NUAA in 2005. His main research directions are new principles, new methods, interdisciplinary, key technologies and integrated innovation research in the fields of helicopter aerodynamics, computational fluid dynamics (CFD), aerodynamic noise, high-performance rotor design, new concept UAV design, stealth design and active flow control.

Author contributions Mr. **REN Binwu** designed the study, conducted the analysis, interpreted the results, and wrote the manuscript. Mr. **CUI Zhuangzhuang** complied the models. Prof. **XU Yousong** tested the content and data of the paper. Prof. **DU Siliang** revised the paper content and data presentation. Prof. **ZHAO Qijun** contributed to the discussion and background research route of this study. All authors commented on the manuscript draft and approved the submission.

Competing interests The authors declare no competing interests.

(Production Editor: SUN Jing)

基于隐模型和LADRC的直升机机动轨迹跟踪控制

任斌武[1],崔壮壮[1],徐尤松[1],杜思亮[2],招启军[1]

(1.南京航空航天大学直升机动力学全国重点实验室,南京 210016,中国;
2.淮阴工学院机械与材料工程学院,淮安 223003,中国)

摘要:为提升直升机执行任务时机动动作的稳定性,设计了基于隐模型(Implicit model, IM)和线性自抗扰(Linear active disturbance rejection control,LADRC)的直升机复合轨迹跟踪控制器。首先,采用叶素理论和均匀入流假设建立了旋翼和尾桨的气动模型。通过拟合机身气动力建立了全机飞行动力学模型。其次,针对直升机的定点盘旋、盘旋上升和莱维斯曼机动进行准定常配平,并在配平处进行小扰动线性化。结合线性化模型,建立了直升机IM姿态内回路和LADRC位置外回路的控制器。最后,将IM-LADRC的机动动作轨迹跟踪结果与经典PID控制方法轨迹跟踪结果进行对比。结果表明,采用配平后小扰动线化模型并结合IM-LADRC的方式能够达到更高精度的跟踪结果,提高了直升机执行机动任务准确性。

关键词:直升机;轨迹跟踪;隐模型;PID;线性自抗扰;小扰动线化;盘旋上升;莱维斯曼